Edge density profile measurements by amplitude modulation reflectometry on PBX-M tokamak

1995 Plasma Phys. Control. Fusion 37 925

(http://iopscience.iop.org/0741-3335/37/9/001)

Plasma Phys. Control. Fusion 37 (1995) 925–935. Printed in the UK

Edge density profile measurements by amplitude modulation reflectometry on PBX-M tokamak

E de la Luna†, G Hanson‡, J Sánchez†, J B Wilgen‡, V A Zhuravlev†, M Ono§ and R Kaita§

† Asociación EURATOM/CIEMAT, 28040 Madrid, Spain
‡ Oak Ridge National Laboratory, Oak Ridge, Tennessee, USA
§ Plasma Physics Laboratory, Princeton University, Princeton, NJ 08543, USA

Received 2 December 1994, in final form 27 April 1995

Abstract. A reflectometer, based on the amplitude modulation technique, has been developed and operated on a PBX-M for the measurement of electron density profile. The system, operating with the extraordinary mode in the range of 32–50 GHz, is able to measure the density profile in the plasma edge from the scrape-off layer up to typically $r/a = 0.7$. The determination of the time delay for each frequency is achieved by measuring the phase delay of a 200 MHz amplitude modulation envelope superimposed on the millimetre wave probing signal. The system has a final bandwidth of 40 kHz and is able to obtain the edge profile during a 1 ms sweep of the microwave source. High quality profiles are obtained in systematic good agreement with Thomson scattering measurements. The profile reconstruction from the raw data is direct, with only a need for minimal data processing. Profiles have been measured for ohmic, RF and NBI heated discharges. Features of the profile changes in the L–H transition are shown. One of the goals of the instrument has been the measurement of the slight modifications to the edge density profile produced by the injection of ion Bernstein waves. These changes have been clearly observed and are in agreement with theoretical expectations.

1. Introduction

Reflectometry has become a promising experimental technique for the measurement of the electron density profile in thermonuclear plasma devices. Its good spatial (≈ 1 cm) and temporal ($\leqslant 100\ \mu$s has been achieved) resolution, together with the moderate access requirements and its ability to perform profile inversion along a single line of sight (avoiding multichord tomography) are very attractive for reactor-like devices. In addition, microwave components close to the machine show acceptable resistance to the effects of radiation.

The relevant quantity in the determination of the density profile by reflectometry is the time delay τ (or differential phase delay, $\tau = (1/2\pi)(\partial\phi/\partial f)$ which the microwave beam undergoes when launched and reflected at the cutoff layer. The profile inversion is performed if $\tau(f)$ is known for a given set of frequencies covering the radial range from the edge to the point of interest. Most profile reflectometers determine $\partial\phi/\partial f$ by measuring the time derivative $\partial\phi/\partial t$ during the sweep of the incident wave frequency. This frequency sweep can be narrow or broadband. This method has shown good results in several experiments (Simonet 1985, Bottolier-Curtet and Ichtchencko 1987, Anabitarte *et al* 1988, Doyle *et al* 1990, Manso *et al* 1991, 1993, Sips *et al* 1992, Paume *et al* 1992, Sips and Kramer 1993) and offers good prospects, but suffers some important limitations. Most experiments which use fringe counters observe a significant number of discharges where the tracking of the phase delay is lost. Turbulence close to the reflecting layer is considered to be the main cause for these disturbances. The reflecting layer moves on a fast time scale, leading to fast phase changes, and additional perturbations are caused by speckle-like phenomena due to the reflection from a corrugated reflecting surface. The 'phase-runaway' phenomena (Bulanin and Korneev 1992, Sánchez *et al* 1992a), which are believed to be caused by poloidal rotating structures in the plasma, can also introduce errors by adding spurious phase shifts to the measurement. Turbulence is stronger at the plasma edge and therefore most failures of reflectometers correspond to this area, where many interesting plasma physics phenomena take place.

Amplitude modulation (AM) reflectometry (Vershkov and Zhuravlev 1987, Sánchez *et al* 1992b, de la Luna *et al* 1993, Stek and Irby 1994) and two-frequency differential-phase reflectometry (Hanson *et al* 1994a) are both differential-phase measurements in that they perform an instantaneous measurement of $\partial\phi/\partial f$ by launching two or more frequencies simultaneously. This method greatly reduces the multiplicity of fringes and minimizes the phase fluctuations in the measured signal resulting from density fluctuations in the plasma.

In this paper we report the first density profiles obtained routinely with the AM technique, corresponding to the edge region of the PBX-M tokamak. After briefly introducing the fundamentals, advantages and drawbacks of the technique, the experimental system is described. Results obtained in NBI, RF and ohmically heated discharges will be shown together with the analysis of the profile modification during the L–H mode transition.

One of the aims of this experiment was the observation of perturbations in the edge density ion Bernstein wave (IBW) heating. The AM reflectometer has been able to measure those small perturbations which are expected from theoretical calculations and can play an important role in the coupling of the IBW power to the plasma. Finally we will draw some conclusions.

2. Amplitude modulation and reflectometry

AM reflectometry uses a microwave probing beam, corresponding to the cutoff frequencies in the plasma (32–50 GHz for extraordinary mode in PBX-M), which is sinusoidally modulated at a lower frequency (200 MHz for this experiment). The resulting spectrum includes the carrier at the original frequency and two sidebands, separated from the carrier by the modulation frequency. The phase delay between the modulating envelopes of the launched and received beams is a direct measurement of the average differential phase shift $\partial\phi/\partial f$ between the resulting carrier and each of the sidebands.

The main advantage of AM reflectometry is the use of a longer equivalent wavelength (that corresponding to the modulation frequency), leading to moderate phase shifts in the final phase meter. The selection of the modulation frequency is based on some physical scale lengths, i.e. the radial correlation length of the density fluctuations, and the scale length of magnetic field gradient (Hanson *et al* 1995, Mazzucato and Nazikian 1995). Another issue which must be considered is the accuracy at which the phase can be measured. The modulation frequency chosen cannot be so small that the errors in the phase measurement are significant relative to the total measured phase.

In addition, the AM measurement is instantaneous, so no phase error is introduced by 'phase-runaway' effects or fast temporal fluctuations during sweeping. AM systems perform a frequency sweep only for probing different plasma positions but not for the determination of the group delay. Therefore multichannel AM reflectometers might operate without the need for sweeping.

The main drawback of AM reflectometry is that the pure AM measurement is only possible when parasitic reflections are absent. This can be overcome by using a two antenna system. In this case, multiple reflections in waveguides or in the plasma are not a severe problem: they lead to a beat (homodyne-like) ripple in the signal which can be filtered out. A discussion about the advantages and limitations of AM reflectometry can be found in the work by Sánchez *et al* (1992b).

In parallel with the AM and the two-frequency differential-phase technique, other approaches based on simultaneous launching of a broad spectrum of frequencies have been developed. These include pulse radar systems, developed by several groups (Hugenholtz and Heijnen 1991, Luhmann *et al* 1994, Shevchenko *et al* 1994) and pulse compression radar (Millot 1992, Laviron 1994). These techniques also have the aim of overcoming the effects of turbulence. AM and two-frequency systems use a simple spectrum and are not affected by higher-order terms in the dispersion relation ($\partial^2\phi/\partial f^2$, $\partial^3\phi/\partial f^3$, etc), but for the same reason, can be disturbed by parasitic reflections. Pulse radar techniques use a broad spectrum and are able to discriminate different reflection points, but might suffer a loss of spatial resolution due to the higher-order dispersion terms which can be generated by plasma turbulence.

3. Experimental system

The system installed on the PBX-M tokamak ($R_0 = 1.65$ m, $a = 0.3$ m, $B = 1.2$–1.5 T, $I = 100$–200 kA), operates in the range of 32–50 GHz, using the extraordinary mode. This frequency band corresponds to densities below 1.5×10^{19} m^{-3}. The reflectometer views the plasma through two 'hog-horn' type antennae, located at the plasma midplane, close to one of the two IBW antennae.

The reflectometer (see figure 1) uses two active frequency-doublers to multiply the 8.0–12.5 GHz input signal to the 32–50 GHz range of interest. The 32–50 GHz millimetre beam is sine-wave modulated by a PIN switch at 200 MHz. The received signals from the plasma and from the reference arm are demodulated in independent biased detectors. Then both signals are amplified and downconverted to a 1 MHz carrier by mixing with a local oscillator at 199 MHz.

The use of a reference arm instead of taking just a reference signal from the modulator driver avoids the distortion introduced by the phase shift generated at the modulator, which might be dependent on the millimetre wave frequency. Both 1 MHz outputs are filtered (40 kHz band pass) and then passed to limiting amplifiers before being compared in the I/Q phase meter to provide the $-\pi$ to π and 0 to 2π outputs. The limiting amplifiers are a very important part of the detection system, they were specially designed for low AM–PM conversion: 0.01 degree per dB of compression at 1 MHz. An amplitude monitor is also available in order to detect when the signal falls below the dynamic range of the system. This signal is very useful in order to tag those parts (if any) in a profile which might include errors. The overall phase error due to the limiting amplifiers and to the receiver noise was kept below 1 degree (corresponding to 2 mm in free space) for operating conditions similar to those during plasma experiments.

The use of a linear phase meter allows for a direct reading of the time delay, but they have a limitation when we want to distinguish fringe transitions from phase fluctuations (see de la Luna *et al* 1994, for a discussion). Due to the modulation frequency of 200 MHz chosen for PBX-M, fringe transitions in the phase meter were mainly due to turbulence. In low turbulence discharges the whole phase delay of the modulating envelope was kept within a fringe of the phase meter during the sweep of the carrier frequency. For experiments which would require a higher dynamic range in the phase meter the best solution is the simultaneous

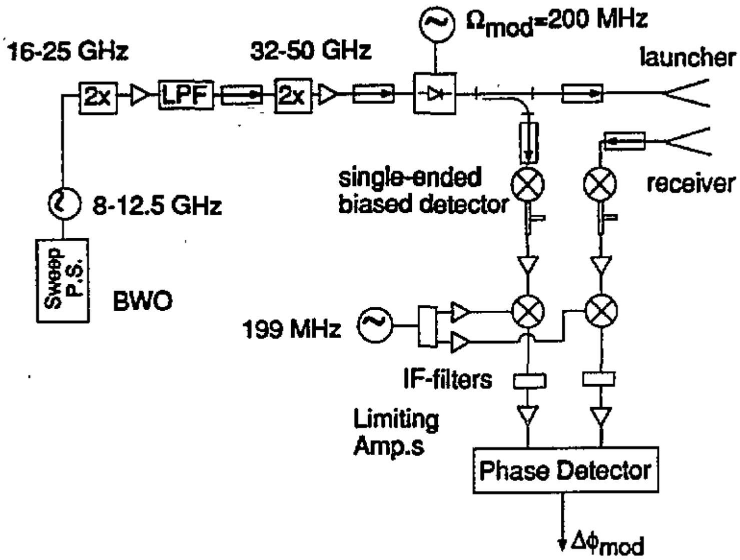

Figure 1. Set-up of the AM reflectometer installed in PBX-M.

use of several modulation frequencies with independent phase meters (for example 50, 100, 200 MHz). The lowest frequency system gives the absolute time delay with low accuracy and the systems operating at higher frequencies add the required final accuracy. Sin–cos phase meters lead to a more indirect determination of the phase, but show the advantage of being able to deal with fast fluctuations present in the time delay.

To allow for testing and calibration, a switchable bypass loop has been installed with a length carefully set to match the waveguide length to the antennae. The bypass loop calibration was tested against an *in situ* calibration using a reflector in front of the antennae during a vacuum opening of PBX-M.

The described system shows high reliability and, due to its simplicity, has low maintenance and investment requirements. Large devices with long runs of waveguide would require heterodyne detection in order to obtain the necessary signal-to-noise ratio. Those systems could generate the multiple frequency spectrum either by using several simultaneous oscillators (Hanson *et al* 1994) or by AM modulation and balanced heterodyne detection (Estrada *et al* 1994). The latter method performs amplification of the carrier after the heterodyne down conversion and before mixing the spectrum, thus avoiding the large dynamic range that direct mixing AM needs (the necessary dynamic range is usually twice that of a homodyne swept reflectometer, since both the carrier and the sidebands come from the probing signal in the direct AM system).

3.1. Experimental results

One density profile is obtained every 5 ms, the sweep time is 1 ms and 4 ms are left between sweeps in order to avoid overheating of the 8–12.5 GHz sweeper. The data acquisition system operates at 500 ks s^{-1}: 512 points per profile are stored. Since the time delay or differential phase delay, $\tau = \partial\phi/\partial\omega$, as a function of the incident frequency, is calculated directly from the phase delay of the modulation signal ($\tau = \Delta\phi/\omega_{\rm mod}$), the profile reconstruction can be performed with no need for sophisticated numerical filtering or signal processing of the raw data. The only filtering used is the 1 MHz bandpass filter, with a 40 kHz bandwidth, located in front of the limiting amplifiers. A numerical algorithm is used (Bottolier-Curtet 1986) to reconstruct the density profile. Though for safety, we took originally a factor of 8 oversampling, in most experiments only one point of every five is taken for the reconstruction process, saving computing time for the profile inversion.

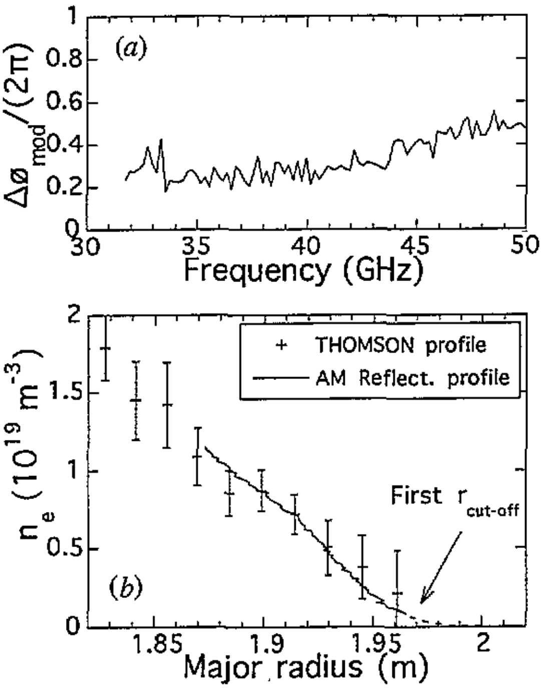

Figure 2. (*a*) AM reflectometry signal (raw data) after subtracting the calibration phase date (B_T = 1.27 T). (*b*) The reconstructed density profile plotted with the Thomson scattering profile for the same time interval.

Figure 2(*a*) shows the phase data for an ohmically heated discharge, once the calibration signal has been subtracted, and figure 2(*b*) shows the density profile obtained by direct inversion of the data shown in figure 2(*a*). The density profile for the range outside the first cutoff is assumed to have an exponential-like decay. Note that the noise in the raw data (figure 2(*a*)) is larger than the noise in the reconstructed density profile (figure 2(*b*)). This effect arises from the mathematical relationship between the time delay and the corresponding profile: the time delay shows a high sensitivity to small profile structures. The density profile is compared with the Thomson scattering profile for the same instant, and both profiles are in quite good agreement.

The problem of profile initialization is common to other technical approaches in reflectometry (swept frequency, pulse radar, etc). Ordinary mode systems have too long wavelengths at the edge, therefore it becomes difficult to go below 5×10^{18} m^{-3} (20 GHz, $\lambda = 1.5$ cm). On the other hand, extraordinary mode systems need an accurate knowledge of the edge magnetic field, since the cutoff layer for low densities is very close to the electron-cyclotron resonance. In PBX-M, the magnitude of the poloidal field was taken into account. The inaccuracy in the calibration of the actual value of the magnetic field in PBX-M could lead to a global shift in the edge profile smaller than 5 mm. The systematic shift would remain almost constant during the transient phases studied in this work and will have very little variation for different discharges. If available, the use of matching points with edge or SOL diagnostics (Langmuir probes, Li/He beam) is very helpful.

Similar data are shown in figure 3 for NBI discharges at different magnetic fields and

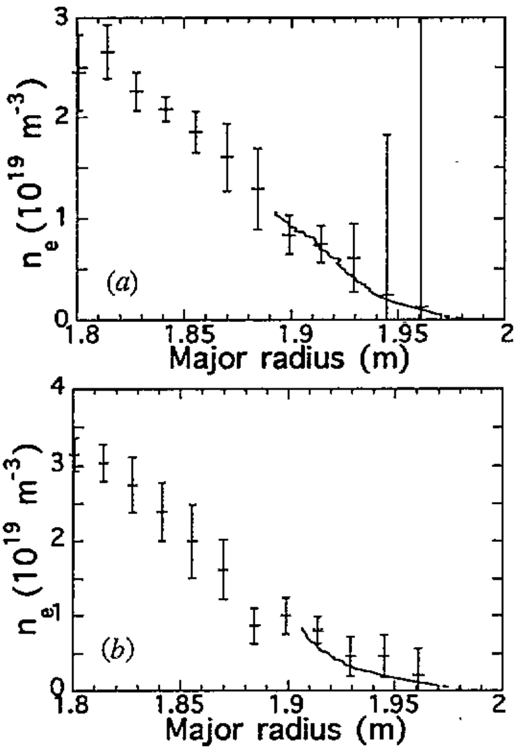

Figure 3. Reconstructed density profiles for neutral beam heated discharges: (*a*) $P_{NB} = 1$ MW, $B_T = 1.31$ T, and (*b*) $P_{NB} = 2.4$ MW, $B_T = 1.45$ T.

power levels, again the agreement with Thomson scattering data is very good.

In figure 4 the evolution of the edge density profile during the L-H transition is described. Figure 4(*a*) shows the time evolution of the Dα signal, the profiles closer to the transition correspond to -1.5 ms and $+3.5$ ms with respect to the first observable change in the Dα signal. The raw data for the two sweeps of interest already show a clear change in the differential phase delay (figure 4(*b*)). The density profiles corresponding to these time intervals, together with the one measured 22.5 ms after the drop in the Dα signal, are plotted in figure 4(*c*). A slight inverted slope of the density profile is seen for the highest densities where the gradient is close to vertical, it might be due to changes in the profile during sweeping caused by the recent transition. The data from the fast reciprocating Langmuir probe, also plotted in figure 4(*c*), are in good agreement with the reflectometer profiles for both L and H phases.

The position of the first reflecting point is shown in the figure, an exponential decaying profile is assumed up to this point. Since the dispersive effects, associated with the local density gradient, represent the largest contributions to the measured phase delay, the uncertainty in the location of the first cutoff position will essentially not change the reconstructed density profile, i.e. shifting this point by one or two centimetres would displace the profile by the same distance without significant modifications in the profile shape.

A relevant observation is that the density gradient already reaches its maximum value (from 2 to 5×10^{20} m^{-4}) in the measurement taken 3.5 ms after the L–H transition, establishing a density profile which remains almost stationary during the H-phase (a trend to move back towards the L-mode profile is observed as the Dα signal increases). This time of 3.5 ms is clearly smaller than the particle confinement time in PBX-M. The observation suggests that the L–H transition in these discharges could be caused by a change in the transport properties over a larger radial region than just a local edge barrier.

A detailed analysis of the edge density profile during the transition is of high interest to understand the process. Unfortunately, the time resolution of the system is not good enough for a detailed study of the transition. This resolution is a consequence of the type of sweeper (1 ms sweep every 5 ms) and the bandwidth of the IF receiver used for this particular experiment, but large improvements can be obtained with existing technology: faster sweepers (systems up to 10 μs sweep time are now available), higher final IF (1 MHz for the PBX-M system), large bandwidth at the last phase meter and an increase in sensitivity in order to keep a high enough signal-to-noise ratio (heterodyne detection might be required). Data acquisition requirements would be moderate, since the ratio of the number of data points in the raw data to the number of final data points in the profile is very favourable when linear phase meters are used. For example, a 100 points profile in 10 μs would require three channels, taking just 100 points each at 10 Ms s^{-1}.

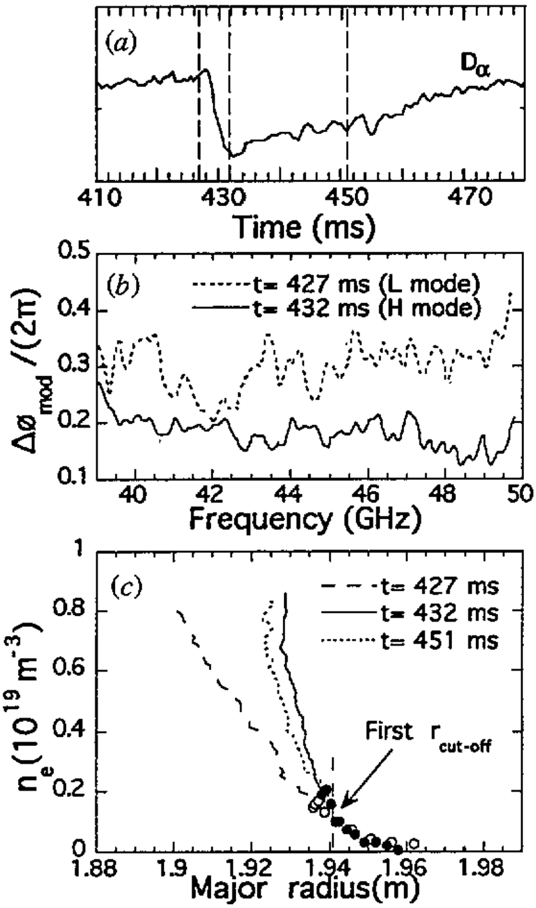

Figure 4. (*a*) Time evolution of the Dα signal during an L–H transition. (*b*) AM phase data for the two sweeps closest to the transition. (*c*) Density profiles measured during the L–H transition. The symbols correspond to data obtained with a reciprocating Langmuir probe (full circles = L-mode, open circles = H-mode).

A possible limitation to the time resolution of most reflectometers measuring density profiles would be the need for averaging due to spatial and temporal turbulence in the density profile: in addition to the fact that some physics studies would be required to operate with 'average profiles' where fast turbulence structures have been smoothed, the spatial corrugated structure of the reflecting layer could lead to phase errors (Nazikian and Mazzucatto 1995) and deformations in the measured profiles. Taking advantage of the temporal evolution of the corrugated surface, a time average would be a possible way to obtain a correct average profile.

In the PBX-M experiment no averaging of multiple sweeps was necessary for the determination of the density profile, but if the sweep time becomes shorter, the problem might appear. It is very difficult to make accurate estimates of this effect from theoretical analysis, and therefore experiments together with cross check with other density profile diagnostics will be necessary to evaluate the limitations.

3.2. Profile modification during IBW heating

One of the goals of the PBX-M reflectometer was the study of the possible perturbations in the edge density profile caused by the application of ion Bernstein wave (IBW) heating. Bulk ion heating and improvement of the particle and energy confinement have been observed in several IBW heating experiments (see Ono 1993, for a review).

For IBW heating, a launched electron plasma wave (EPW) is converted by mode transformation into the ion Bernstein wave, which theoretically has better accessibility to the hot dense plasma core. This process is critically dependent on the edge plasma density immediately in front of the antenna. When the density in front of the antenna is sufficiently high, such that $\omega_{rf} < \omega_{lh} \approx \omega_{pi}$, direct IBW coupling can occur. In the opposite case, i.e. the low edge density regime, where $\omega_{rf} > \omega_{pi}$, the antenna is coupled to the EPW, which smoothly connects to the IBW near $\omega_{rf} \approx \omega_{pi}$ (mode transformation). These two regimes show different dependences for the antenna loading. In the EPW regime the magnetic field dependence is relatively weak, while in the direct IBW coupling regime, the antenna loading peaks strongly when a cyclotron resonance layer appears close to the antenna.

The density in front of the antenna, and therefore the coupling, can be affected by the IBW itself. Since the IBW coupler is oriented along the toroidal direction, the ponderomotive force associated with the antenna near fields ($E_{\parallel} \sim 300$ V cm^{-1}) can be quite large. Under these conditions, one can expect a significant plasma density reduction in front of the antenna which can lead to nonlinear effects.

The perturbed density due to the ponderomotive force can be estimated as

$$n = n_0 \exp(-\Psi_{rf}/(T_e + T_i)) \tag{1}$$

where

$$\Psi_{rf} = \frac{1}{4m_e}\frac{e^2 E_{\parallel}^2}{\omega_{rf}^2} \tag{2}$$

is the ponderomotive potential.

Due to the strong frequency dependence of the ponderomotive potential, this phenomenon is expected to be especially important for low-frequency IBW experiments (10–100 MHz). For the case of the PBX-M, with $f_{rf} = 54$ MHz, Ψ_{rf} can be of the order of 1 keV for moderate power levels, which is greater than the edge plasma temperature and therefore it can produce a substantial density depletion.

The modification of the IBW antenna coupling due to the ponderomotive potential has been investigated previously for the lower-hybrid wave case (Wilson and Wong 1982, Leuterer *et al* 1991), and has also been observed for the IBW case in the ACT-1 (Skiff 1985), DIII-D (Mayberry *et al* 1993) and PBX-M (Jiang *et al* 1991) tokamaks. No dependence of the antenna coupling with the toroidal magnetic field was found in the experiments on DIII-D and PBX-M. These results can be explained if the plasma density near the antenna is reduced, avoiding direct IBW coupling. More direct evidence of the plasma reduction in front of the antenna due to the ponderomotive potential was obtained from the measurements of the reactive antenna loading in DIII-D (Mayberry *et al* 1993). It was found that moving the plasma away from the antenna produced a decrease in the measured reactive antenna loading, and the same effect was obtained by raising the RF power. However, no direct measurements of the density modifications has been reported in an IBW heating tokamak experiment.

To investigate this type of phenomena in PBX-M, the reflectometer antennae were installed at $R = 2.02$ m, immediately adjacent to the antenna Faraday shield ($R = 1.97$ m), in order to obtain a direct measurement of the profile modifications during the IBW heating. The parameters of the discharges used were: circular cross sections plasmas, $I = 127$ kA, $B_t = 1.45$ T, and $f_{rf} = 54$ MHz.

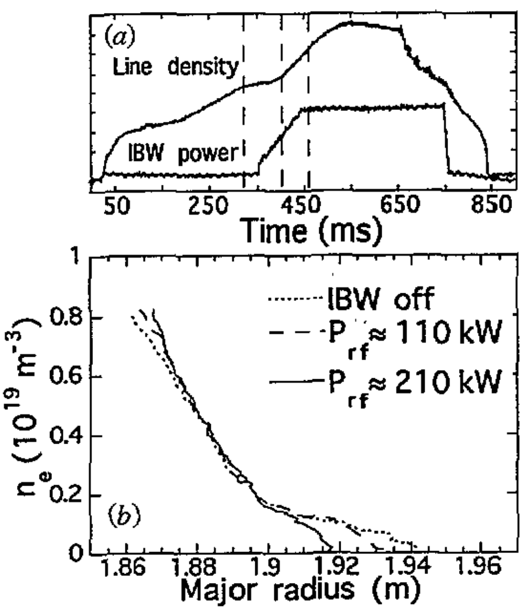

Figure 5. (*a*) Time evolution of the interferometer signal and the IBW power. (*b*) Density profiles measured during the ramp up of the IBW power. For better clarity three consecutive profiles were averaged in the stationary phases.

In figure 5(*b*), the temporal evolution of the edge density profile is plotted for a discharge in which the IBW power was ramped up slowly (over 100 ms) to a final level of 210 kW. It shows how a density 'hole' is developed in front of the antenna, the edge density is reduced and the density gradient is steepened after the RF power is switched on. The plots in figure 5(*b*) have been performed taking the average of three consecutive seeps during the stationary phases (IBW off and 210 kW) and a single sweep during the ramp up phase (110 kW). The averaging is not strictly necessary to observe the effect but it is helpful in order to show a clearer plot. This density depletion grows as the RF power level increases. As one can see from equations (1) and (2), such an effect is not unexpected. Since $|E_\parallel| \propto (P_{rf}/A)^{1/2}$, where A is the antenna surface area, the ponderomotive potential, and therefore, the magnitude of the density perturbation will scale with the RF power. It is also clearly seen how the gradient of the density profile increases, accordingly with the increase in the line density measured by the interferometer.

In order to locate the profiles in the chamber, data from the Thomson scattering have been used for the case with IBW. The density profile for the case without IBW has been initialized to match with the IBW-on profile in the steep gradient region. This method is based on the fact that the effects of the ponderomotive force are expected only to be seen at the very edge of the density profile. The density measured by Langmuir Probe during the IBW is higher than that measured by the reflectometer, but it should be noticed that the edge density measured by the probe (located approximately 2 m from the IBW antenna) does not necessarily correspond to that immediately in front of the antenna, especially at high RF power injection.

4. Conclusions

A reflectometer based in the AM technique has been installed and operated on the PBX-M tokamak. For the first time on a fusion plasma device, density profiles have been routinely obtained with this technique. The system has been able to measure the density profile in OH, NBI and RF heated discharges. The results are in systematic good agreement with Thomson scattering measurements. Initialization of the profile is still a problem, common to other reflectometry techniques, so complementary data from Langmuir probes are helpful. The shape of the profile, once the initial point has been chosen, can be obtained to high accuracy.

Clear profile changes are observed during the L–H mode transition. The AM reflectometry data show that the H-density profile is established in not more than 5 ms after the Dα drop.

The effects of IBW heating on the edge density profile have been studied. A density depletion which appears when the IBW is applied is observed; the magnitude of the density perturbation increases with increasing IBW power. This observation confirms the theoretical expectations that a ponderomotive force is modifying the edge density profile in front of the antenna, leading to changes in the IBW coupling to the plasma.

The PBX-M experiment has shown the viability of AM reflectometry as a mature technique for density profile measurements, with low sensitivity to the effects of turbulence. The existing technology allows for the development of fast AM systems with high time resolution (10–100 μs for a single profile).

Acknowledgments

The authors wish to acknowledge many useful discussion of these results with T K Chu. We thank B LeBlanc for providing us with the Thomson scattering profiles and G Tynan, L Schmitz, L Blush and I García-Cortés for the Langmuir probe data. We particularly appreciate the help of all the members of the PBX-M team during the realization of this work. We would also like to thank J H Harris, J L Dunlap, N Sauthoff and A P Navarro for their support to this project.

This work was sponsored in part by DOE under contracts DE-AC05-84-OR-21400 and DE-AC02-76-CHO-3073 and in part by EURATOM.

References

Anabitarte E, Bustamante E G, Calderón M A G, Senties J M, Navarro A P and Sánchez J 1988 *J. Phys. D: Appl. Phys.* **21** 1384

Bottolier-Curtet H 1986 *PhD Thesis* University of Paris

Bottolier-Curtet H and Ichtchencko G 1987 *Rev. Sci. Instrum.* 58 539

Bulanin V V and Korneev D 1992 *Proc. 1st IAEA Tech. Meeting on Microwave Reflectrometry for Fusion Plasma Diagnostics (Abingdon)* (Oxford: Culham Laboratory) p 184

de la Luna E, Zhuravlev V A, Brañas B, Sánchez J and Estrada T 1993 *Proc. 20th European Conf. on Controlled Fusion and Plasma Physics (Lisboa)* vol 17C (European Physical Society) part III, p 1159 de la Luna E *et al* 1994 *Rev. Sci. Instrum.* **66** accepted

Doyle E J, Lehecka T, Luhmann N C Jr, Peebles W A and the DIII-D Group 1990 *Rev. Sci. Instrum.* **61** 2896

Estrada T *et al* 1994 *Proc. 21st European Conf. on Controlled Fusion and Plasma Physics (Montpellier)* vol 18B (European Physical Society) part I, p 404

Hanson *et al* 1994 *Plasma Phys. Control. Fusion* **36** 2073

Hanson G R, Wilgen J B, Bigelow T S, Collazo I, England A C, Murakami M, Rasmussen D A and Wilson J R 1995 *Rev. Sci. Instrum.* **66** 863

Hugenholtz C A J and Heijnen S H 1991 *Rev. Sci. Instrum.* **62** 1100

Jiang T W *et al* 1991 *Proc. 9th Topical Conf. on Radio-Frequency Power in Plasmas (Charleston, SC)* (New York: American Institute of Physics) p 129

Laviron C *et al* 1994 *Proc. 21st European Conf. on Controlled Fusion and Plasma Physics (Montpellier)* vol 18B (European Physical Society) part III, p 1168

Leuterer F *et al* 1991 *Plasma Phys. Control. Fusion* **33** 169

Luhmann N C *et al* 1994 *Proc. 2nd IAEA Tech. Meeting on Microwave Reflectrometry for Fusion Plasma Diagnostics (Princeton)* (Princeton, NJ: Plasma Physics Laboratory)

Manso M E 1993 *Plasma Phys. Control. Fusion* **35** B141

Manso M E *et al* 1991 *Proc. 18th European Conf. on Controlled Fusion and Plasma Physics (Berlin)* vol 15C (European Physical Society) part I, p 393

Mayberry M J, Pinsker R I, Petty C C, Porkolab M, Chiu S C, Cary W P and Prater P 1993 *Nucl. Fusion* **33** 627

Mazzucato E and Nazikian R 1995 *Rev. Sci. Instrum.* **66** 1237

Millot P 1992 *Proc. 1st IAEA Tech. Meeting on Microwave Reflectrometry for Fusion Plasma Diagnostics (Abingdon)* (Oxford: Culham Laboratory) p 204

Nazikian R and Mazzucato E 1995 *Rev. Sci. Instrum.* **66** 392

Ono M 1993 *Phys. Fluids* **B5** 241

Paume M, Chareau J M, Clairet F and Zou X L 1992 *Proc. 1st IAEA Tech. Meeting on Microwave Reflectrometry for Fusion Plasma Diagnostics (Abingdon)* (Oxford: Culham Laboratory) p 184

Sánchez J, Estrada T and Hartfuss H J 1992a *Proc. 1st IAEA Tech. Meeting on Microwave Reflectrometry for Fusion Plasma Diagnostics (Abingdon)* (Oxford: Culham Laboratory) p 133

Sánchez J, Brañas B, Estrada T, de la Luna E and Zhuravlev V A 1992b *Rev. Sci. Instrum.* **63** 4654

Shevchenko V F, Petrov A A, Petrov V G and Chaplygin Yu A 1994 *Plasma Phys. Rep.* **20** 27

Simonet F 1985 *Rev. Sci. Instrum.* **56** 664

Sips A C C, Kramer G J, Beurskens M, Costley A E and Prentice R 1992 *Proc. 1st IAEA Tech. Meeting on Microwave Reflectrometry for Fusion Plasma Diagnostics (Abingdon)* (Oxford: Culham Laboratory) p 11

Sips A C C and Kramer G J 1993 *Plasma Phys. Control. Fusion* **35** 743

Skiff F 1985 *PhD Thesis* Princeton University

Stek P C and Irby J H 1994 *Proc. 2nd IAEA Tech. Meeting on Microwave Reflectrometry for Fusion Plasma Diagnostics (Princeton)* (Princeton, NJ: Princeton Plasma Physics Laboratory)

Verskov V A and Zhuravlev V A 1987 *Sov. Phys. Tech. Phys.* **32** 523

Wilson J R and Wong K L 1982 *Phys. Fluids* **25** 675